Patients with recurrent PVL^{+}-*Staphylococcus aureus* infections show enhanced sensitivity to PVL-mediated formation of atypical NETs

Authors

Hina Jhelum[1], Dora Čerina[1], CJ Harbort[1], Andreas Lindner[2], Leif Gunnar Hanitsch[3], Rasmus Leistner[4], Jennyver-Tabea Schröder[5], Horst von Bernuth[6,7,8,9], Miriam Songa Stegemann[10], Mariana Schürmann[10], Arturo Zychlinsky[1], Renate Krüger[11*], Gerben Marsman[1*]

* Contributed equally to the manuscript

Author affiliations

[1]Department of Cellular Microbiology, Max Planck Institute for Infection Biology, Charitéplatz 1, 10117, Berlin, Germany

[2]Institute of Tropical Medicine and International Health, Charité, Universitätsmedizin Berlin, Berlin, Germany

[3]Department of Medical Immunology, Charité, Universitätsmedizin Berlin, Berlin, Germany

[4]Institute of Hygiene and Environmental Medicine, Charité, Universitätsmedizin Berlin, Berlin, Germany

[5]Department of Pediatric Surgery, Charité, Universitätsmedizin Berlin, Berlin, Germany

[6]Department of Pediatric Respiratory Medicine, Immunology and Critical Care Medicine, Charité - Universitätsmedizin Berlin, corporate member of Freie Universität Berlin, Humboldt-Universität zu Berlin, and Berlin Institute of Health (BIH), Berlin, Germany

[7]Department of Immunology, Labor Berlin GmbH, Berlin, Germany

[8]Berlin Institute of Health at Charité - Universitätsmedizin Berlin, Germany

[9]Berlin-Brandenburg Center for Regenerative Therapies (BCRT), Berlin Institute of Health at Charité, Universitätsmedizin Berlin, corporate member of Freie Universität Berlin, Humboldt-Universität zu Berlin, and Berlin Institute of Health (BIH), Berlin, Germany

[10]Department of Infectious Diseases and Respiratory Medicine, Charité, Universitätsmedizin Berlin, Berlin, Germany

[11]Department of Pediatric Respiratory Medicine, Immunology and Critical Care Medicine, Charité, Universitätsmedizin Berlin, Berlin, Germany

36

37 **List of abbreviations**

38 CFU	Colony forming unit
39 CGD	Chronic granulomatous disease
40 DAP	Differentially abundant proteins
41 DAPI	4´,6-diamidino-2-phenylindole
42 DHR	Dihydrorhodamine
43 DNP	Dinitrophenol
44 DPBS	Dulbeccos`s phosphate-buffered saline
45 DPI	Diphenyleneiodonium chloride
46 FCCP	Carbonyl cyanide-p-trifluoromethoxyphenylhydrazone
47 FDR	False discovery rate
48 HCD	Higher-energy collisional dissociation
49 HEPES	Hydroxyethyl-Piperazine-Ethane Sulfonic Acid
50 Hlg	γ-Hemolysin
51 HAS	Human serum albumin
52 MFI	Mean fluorescent intensities
53 MPO	Myeloperoxidase
54 MS	Mass spectrometry
55 NE	Neutrophil elastase
56 NEi	Neutrophil elastase inhibitor
57 NETs	Neutrophil extracellular traps
58 PBS	Phosphate-buffered saline
59 PFA	Paraformaldehyde
60 PKC	Protein Kinase C

PMA	Phorbol 12-myristate 13-acetate
PMN	Polymorphonuclear leukocytes
PSMs	Peptide-spectrum-matches
PVL	Panton-Valentine leukocidin
PVL-SA	PVL-positive *S. aureus*
ROS	Reactive oxygen species
RT	Room temperature
S. aureus	*Staphylococcus aureus*
SDS	Sodium Dodecyl Sulfate
SSTI	Skin and soft tissue infections
TCEP	Tris-(2-carboxyethyl)phosphine
TFA	Trifluoroacetic acid
TMM	Trimmed mean of M values
TMT	Tandem Mass Tag

Abstract

Panton-Valentine leukocidin (PVL) is a *Staphylococcus aureus* (*S. aureus*) toxin that binds to and kills human neutrophils, resulting in the formation of neutrophil extracellular traps (NETs). Some individuals colonized with PVL-positive *S. aureus* (PVL-SA) suffer from recurring infections whereas others are asymptomatically colonized. We found that neutrophils from affected patients express higher levels of CD45, one of the PVL receptors, and are more susceptible to killing at a low concentration of recombinant PVL than control neutrophils. We verified that PVL induces the formation of NETs and provide genetic and pharmacological evidence that PVL-induced NET formation is independent of NADPH-oxidase and reactive oxygen species (ROS) production. Through NET proteome analysis we identified that the protein content of PVL-induced NETs is different from NETs induced by mitogen or the microbial toxin nigericin. The abundance of the proteins cathelicidin (CAMP), elastase (NE), and proteinase 3 (PRTN3) was lower on PVL-induced NETs, which were inefficient in killing *S. aureus.* Neutrophils from patients that suffer from recurring PVL-positive infections may be more sensitive to PVL-induced NET formation, which may impair their ability to combat the infection.

Introduction

S. aureus is a widespread Gram-positive pathogen that causes infections in skin and soft tissue (SSTI), osteoarticular, airway, and the blood stream in humans and animals. Nasal colonization with *S. aureus* is found in approximately 50% of humans, with strong age variation, and may be asymptomatic provided that skin and mucous membrane barriers are intact [1,2]. Pathogenicity of *S. aureus* strains depends on a variety of virulence factors, among those, pore-forming leukocidins such as PVL that target neutrophils (also called polymorphonuclear leukocytes, PMN), and macrophages to evade phagocytosis and intracellular killing (reviewed in [3]). Over the last two decades an increasing number of outbreaks of SSTI in close communities [4–12] and in other health care settings [13–24] were caused by *S. aureus* strains that produce PVL (PVL- SA).

Although recurrent deep skin abscesses and furunculosis are the most frequent manifestations of PVL-SA infections, other pathologies are also linked to these strains. These include (a) worldwide reports of severe invasive infections - often complicated by thrombotic events - in previously healthy young individuals [25–27], (b) breast abscesses in lactating women [28] and transmission to offspring that can cause life-threatening infections [29], and (c) necrotizing pneumonia [30], a severe manifestation, often fatal within days of hospital admission [31,32]. In some cases, pneumonia is preceded by viral airway infections, like influenza, parainfluenza [31,32] and SARS-CoV2 [33].

During outbreaks, identical PVL-SA strains have been obtained from individuals with asymptomatic nasal colonization as well as from patients with severe SSTI or invasive infections [11], suggesting that host factors may explain susceptibility to, and severity of, PVL-SA infections. Although studies in African Pygmies suggest that genetic variations in *C5ARI* may be associated with PVL-SA colonization [34], other factors that allow PVL-SA colonization or infections are not known.

The binding specificity of PVL defines both its host- and cell tropism. PVL is a two-component toxin consisting of LukF-PV and LukS-PV, which bind to the human panleukocyte receptor CD45 [35], and the human complement 5a receptors CD88/C5aR and C5L2, respectively [36]. As a result, human phagocytes are the major target of PVL. Upon binding, the subcomponents hetero-oligomerize into an octameric membrane spanning pore [37,38], which drives cell death. Neutrophils express higher levels of both C5a receptors than monocytes [36] and are more

141 sensitive to PVL mediated killing than both monocytes and macrophages [39],
142 suggesting they are the major target of PVL. Importantly, neutrophils form an
143 important cellular host defense against *S. aureus* [40] and patients with impaired
144 production of reactive oxygen species (ROS) in phagocytes are particularly
145 sensitive to *S. aureus* infections (see review [41]). Neutrophils clear invading *S.*
146 *aureus* through phagocytosis and by undergoing NETosis, a cell death process
147 which results in the formation of neutrophil extracellular traps (NETs). NETs consist
148 of an externalized web of chromatin decorated with antimicrobial peptides and
149 proteases and are toxic to bacteria [42].

150 Depending on the stimulus, NET formation may require ROS formation [43]. A
151 common mediator of ROS-dependent NET formation is NADPH-oxidase, which
152 produces superoxide (O^{2-}) that spontaneously dismutates to hydrogen peroxide
153 (H_2O_2). Myeloperoxidase (MPO) converts hydrogen peroxide into highly reactive
154 hypochlorous acid (HOCl). ROS production allows for the release of neutrophil
155 proteases from granules, protease-mediated chromatin decondensation and the
156 final lysis of the plasma membrane [44–46]. Two *S. aureus* toxins that kill
157 neutrophils and result in NET formation are γ-hemolysin AB and PVL [47–49].
158 Interestingly, *S. aureus* also produces nucleases to escape from NETs [50].
159 Whether NET formation is a beneficial or detrimental neutrophil response, both for
160 the host as well as for *S. aureus*, remains unclear and may be context dependent
161 [48].

162 In this study, we show that neutrophils from patients with a history of recurrent
163 PVL-SA infections express higher levels of the PVL receptor CD45 than healthy
164 controls and make more NETs in response to a low concentration of PVL.
165 Furthermore, PVL-induced NET formation is NADPH-oxidase independent.
166 Consistently, neutrophils isolated from chronic granulomatous disease (CGD)
167 patients, which have a mutation in the gene encoding one subunit of the NADPH
168 oxidase complex, make NETs in response to this toxin [51]. PVL-induced NETs
169 showed quantitative proteomic differences to NETs produced after PMA or nigericin
170 stimulation. PVL NETs contained a lower abundance of multiple antimicrobial
171 proteins and did not kill *S. aureus.* Our results suggest that PVL-receptor
172 expression may mediate susceptibility to symptomatic *S. aureus* infection and that
173 NET-formation induced by this toxin serves as an offensive strategy to
174 preemptively neutralize the neutrophil.

175 **Materials and Methods**
176

177 **Patient and control characteristics**

178 Patient demographic and clinical data are summarized in Supplementary Table 1.
179 Controls were matched for gender and age. All study participants provided written
180 informed consent and were free of infections at the time of blood withdrawal. The
181 study was approved by the local Ethics committee (EA2/003/19). Healthy control
182 samples were collected according to the approval and guidelines of the local ethics
183 committee (EA1/0104/06).

184

185 **Neutrophil isolation, experimental conditions, and inhibitors**

186 Human neutrophils were isolated by layering whole blood over Histopaque-1119
187 (Sigma) followed by a discontinuous Percoll gradient (Amersham Biosciences) as
188 previously described [45]. Alternatively, they were also isolated using the direct
189 human neutrophil isolation kit (EasySep, StemCell Technologies) following
190 manufacturer´s instructions. All experiments were performed in Seahorse XF RPMI
191 medium (SF-RPMI, Agilent) supplemented with 2 mM glutamine, 10 mM HEPES, 1
192 mM glucose and 0.1% human serum albumin (HSA) at pH 7.4 except where
193 mentioned. The stimuli used to induce NET formation were phorbol 12-myristate
194 13-acetate (PMA, Sigma), PVL (equal amounts of *S. aureus* recombinant LukS and
195 LukF (Bioservices), and nigericin (InvivoGen). We used the following inhibitors:
196 Gö6983 (PKCi, Tocris) BAPTA-AM (Thermo Fisher Scientific), pyrocatechol
197 (Sigma), 4-Aminobenzoic acid hydrazide (ABAH, Cayman chemical), neutrophil
198 elastase inhibitor (NEi, MedChemExpress), Diphenyleneiodonium chloride (DPI,
199 Calbiochem), AEBSF (Sigma), allopurinol (Sigma), Apamin (Sigma), 2,4-
200 Dinitrophenol (DNP, Sigma) and 2-[[4-(trifluoromathoxy) phenyl]hydrazinylidene]
201 propanedinitrile (FCCP, Abcam).

202

203 **Neutrophil markers**

204 $1x10^6$/ml neutrophils were fixed for 15 min using 4% PFA and washed to PBS
205 supplemented with 0.1% HSA. Cells were incubated with anti-CD63-PE, anti-
206 CD66b-APC (Miltenyi Biotec), 5 µg/ml anti-CD45-AlexaFluor 647 (Santa Cruz
207 Biotechnology), 10 µg/ml CD88 (S5/1)-FITC (Santa Cruz Biotechnology) and 10

208 μg/ml anti-human C5L2-APC (BioLegend) antibodies for 30 min in the dark,
209 washed thereafter to PBS supplemented with 0.1% HSA and measured on a
210 CytoFLEX (BeckMan Coulter) or MACSQuant (Miltenyi Biotec).

211

212 **ROS measurement**

213 Purified neutrophils were seeded at 10^5 cells per well in a 96-well plate and
214 incubated for 30 min with the indicated inhibitors, followed by incubation for 10
215 min with 50 μM luminol and 1.2 units/ml horseradish peroxidase at 37°C prior to
216 stimulation with indicated stimuli. Luminescence was measured over time in a
217 VICTORX luminometer (Perkin Elmer) [43].

218

219 **Neutrophil lytic cell death assay**

220 10^5 neutrophils were seeded in a 96-well plate and incubated with the appropriate
221 inhibitors for 30 min, followed by incubation with 50 nM cell-impermeable DNA dye
222 SYTOX Green (ThermoFisher Scientific) for 5 min at 37°C, prior to stimulation with
223 indicated stimuli. Fluorescence was recorded once per hour for 4h using a
224 Fluoroskan Ascent (ThermoFisher Scientific).

225

226 **NET staining**

227 10^5 neutrophils were seeded on glass coverslips in a 24-well plate and incubated
228 with or without appropriate inhibitors followed by stimulation with indicated stimuli
229 for 4 h at 37°C. Cells were fixed with 4% paraformaldehyde (PFA) for 20 min at
230 room temperature. Cells were washed with PBS, permeabilized with 0.5% Triton
231 X-100 for 1 min and incubated in blocking buffer (3% normal goat serum, 3% cold
232 water fish gelatin, 1% bovine serum albumin and 0.05% Tween-20 in PBS) for 30
233 min. Neutrophils were then stained using antibodies detecting elastase (Merck
234 Millipore, 481001) and a subnucleosomal complex of Histone 2A, histone 2B and
235 chromatin (Losman et al., 1992; in-house generated). The secondary antibodies
236 used were goat anti-mouse Alexa Fluor 488 (Invitrogen, A11029) and goat anti-
237 rabbit Alexa Fluor 647 (Invitrogen, A21245) followed by staining with DAPI (0.1
238 μg/ml, Invitrogen). Finally, the samples were mounted using antifade mountant

239 (ProLong Diamond Antifade mountant, ThermoFisher Scientific). Images were
240 acquired using a Leica TCS SP8 confocal microscope.

241 For live NET imaging, cells were resuspended in Agilent XF RPMI medium (Agilent)
242 at pH 7.4, supplemented with 0.1% Human Serum Albumin, 10 mM Glucose
243 (Sigma Aldrich), 2 mM L-Glutamine (Gibco), 20 mM HEPES (Gibco) 500 nM SYTOX
244 Green (Thermo Fischer) and 2.5 µM DRAQ5 (Biostatus) and seeded at a density of
245 $5x10^5$ cells per well into µ-slide 8 well ibiTreat dishes (ibidi). Cells were stimulated
246 with final concentrations of 100 nM PMA and 10 nM PVL. Images were collected at
247 2 min intervals on a Leica TCS SP8 confocal microscope equipped with a climate
248 chamber at 37°C and with a Leica HC PL APO 20x/0.75 IMM CORR CS2 objective
249 using glycerol immersion [43].

250

251 **Phagocytosis assay**

252 $1x10^6$/ml neutrophils were incubated with $10x10^6$/ml AlexaFluor 488-labeled
253 *Escherichia coli (E. coli)* particles (ThermoFisher Scientific) in RPMI supplemented
254 with 5% human pooled serum (Sigma) for 30 min on a rotator. Cells were fixed
255 for 15 min using 4% PFA and separated from non-phagocytosed particles by
256 centrifugation at 200x *g* for 10 min. Cells were washed with PBS supplemented
257 with 0.1% HSA and phagocytosis was quantified by flow cytometry on a Cytoflex
258 (Beckman Coulter) or MACSQuant (Miltenyi Biotec).

259

260 **Mass spectrometry (MS)**

261 Human neutrophils from three different healthy donors were seeded in 6-well
262 tissue culture plate to a density of $3x10^5$ cells per well (SF-RPMI without HSA) and
263 then stimulated with 50 nM PMA, 10 nM PVL, or 15 µM nigericin for 4 h to induce
264 NETs. As a control, neutrophils were incubated in medium for 4 h. Media was
265 carefully removed followed by a wash with fresh media to remove unbound
266 proteins. NETs were collected by treatment with lysis buffer (1% SDS, 50 mM
267 HEPES pH 8, 10 mM tris-(2-carboxyethyl)phosphine (TCEP), 40 mM
268 Chloroacetamide and protease-inhibitor cocktail) and subsequent scraping.

269 All samples were subjected to SP3 sample preparation [52]. Briefly, proteins were
270 denatured, reduced and alkylated, and subsequently digested with Trypsin and

271 Lys-C proteases. TMT 11plex (Pierce) labelling was used for peptide multiplexing
272 and quantification. Samples were mixed, desalted using solid phase extraction
273 (Seppak 1cc/50 mg, Waters), and fractionated using basic reversed phase
274 fractionation on a quaternary Agilent 1290 Infinity II UPLC system equipped with
275 a Kinetex Evo-C18 column (150 x 2.1 mm, 2.6µm, 100 Å, Phenomenex). Fractions
276 were concatenated into 8 final samples, dried down and resuspended in 2%
277 acetonitrile, 0.1% trifluoroacetic acid (TFA) prior MS analysis. All samples were
278 analyzed on an Orbitrap Q Exactive HF (Thermo Scientific) that was coupled to a
279 3000 RSLC nano UPLC (Thermo Scientific). Samples were loaded on a pepmap trap
280 cartridge (300 µm i.d. x 5 mm, C18, Thermo) with 2% acetonitrile, 0.1% TFA at a
281 flow rate of 20 µL/min. Peptides were separated over a 50 cm analytical column
282 (Picofrit, 360 µm O.D., 75 µm I.D., 10 µm tip opening, non-coated, New Objective)
283 that was packed in-house with Poroshell 120 EC-C18, 2.7 µm (Agilent). Solvent A
284 consists of 0.1% formic acid in water. Elution was carried out at a constant flow
285 rate of 250 nL/min using a 180-minute method: 8-33% solvent B (0.1% formic
286 acid in 80% acetonitrile) within 120 minutes, 33-48% solvent B within 25 minutes,
287 48-98% buffer B within 1 minute, followed by column washing and equilibration.
288 The mass spectrometer was operated in data-dependent acquisition mode. The
289 MS1 survey scan was acquired from 375-1500 m/z at a resolution of 120,000. The
290 top 10 most abundant peptides were isolated within a 0.7 Da window and
291 subjected to HCD fragmentation at a normalized collision energy of 32%. The AGC
292 target was set to 2e5 charges, allowing a maximum injection time of 78 ms.
293 Product ions were detected in the Orbitrap at a resolution of 45,000. Precursors
294 were dynamically excluded for 45 s. Raw files were processed with Proteome
295 Discoverer 2.3 (Thermo Scientific) using SEQUEST HT for peptide identification.
296 Peptide-spectrum-matches (PSMs) were filtered to a 1% false discovery rate (FDR)
297 level using Percolator employing a target/decoy approach. The protein FDR was
298 set to 1%. Further data processing was carried out in R and Perseus (v. 1.6.2.3).
299 Only proteins identified with at least two peptides were included in the analysis.
300 All contaminant proteins were filtered out. A three-step normalization procedure
301 was applied. First, the total intensity of each TMT channel was normalized to
302 correct for mixing errors. Next, the common channel in both TMT sets was used
303 for internal reference scaling [53] in order to correct for batch effects. Afterwards
304 the data was normalized applying trimmed mean of M values (TMM) using the
305 edgeR package in R [54]. Proteins were filtered on those detected in at least two

306 of three replicate experiments. Remaining undetected (NA) values were replaced
307 with the sample-wise minimum abundance as an estimation of the limit of
308 detection. Differential protein abundances were calculated using the limma
309 package in R [55]. Principle component analysis and calculation of Euclidean
310 distance between proteome samples were performed using scaled
311 log2(abundance) values.

312

313 **NET killing assay**

314 Isolated neutrophils were resuspended in RPMI supplemented with 10% human
315 serum (Sigma). 10^6 neutrophils were seeded in a flat-bottom 96-well plate, and
316 NETosis was induced for 3 h at 37 °C, 5% CO_2 with 100 nM PVL or 200 nM PMA.
317 *S. aureus* (USA300) in mid-logarithmic phase was resuspended in RPMI with 10%
318 human serum and added to each well at a multiplicity of infection of 0.1. Bacteria
319 were spun down for 5 min at 1500 x g and incubated for 1 h at 37 °C after which
320 the NETs were treated with 2 U Micrococcal nuclease from *S. aureus* (Sigma) for
321 10 min at RT. Subsequently, the samples were serially diluted in DPBS and plated
322 on trypticase soy agar plates. The plates were incubated overnight at 37 °C and
323 colony-forming units were counted.

324 For DNA quantification, 10^6 neutrophils were seeded in plates and NETosis was
325 induced as described above. NETs were digested with 2 U micrococcal nuclease for
326 10 min at RT, and subsequently with 0.5 mg/ml of proteinase K (Invitrogen) for 1
327 h at 50°C. The samples were vortexed and the DNA concentration was determined
328 by measuring absorbance at 260 nm on a Nanodrop 2000 spectrophotometer
329 (ThermoFisher Scientific).

330

331 **Statistical analysis**

332 Analysis of differential protein abundance was performed in limma (Linear Models
333 for Microarray data) in R, which has been shown to outperform t-tests in detecting
334 significant changes in protein abundance [56]. Protein-wise linear models were fit
335 and batch-corrected using the formula (0 + condition + batch) and significant
336 changes in abundance were tested using an empirical Bayes moderated t-statistic
337 with Benjamini-Hochberg correction. Changes in abundance were considered
338 significant at an absolute log2 fold change > 1, and an adjusted p value < 0.01.

339 Euler diagrams of significant changes across samples were visualized with the
340 eulerr package [57]. Significant proteins were clustered by pattern across
341 conditions using k-means clustering with indicated number of clusters. Heatmaps
342 were produced using pheatmap package [58].

343 R scripts for proteome analysis and visualization are available upon request and
344 will be made publicly available upon publication.

345 Data are represented as mean±SD unless otherwise stated.

346

347 **MS data availability**

348 The mass spectrometry proteomics data have been deposited to the
349 ProteomeXchange Consortium via the PRIDE [59] partner repository with the
350 dataset identifier PXD025702.

351 Reviewer account details:

352 **Username:** reviewer_pxd025702@ebi.ac.uk

353 **Password:** Yr3cVMPZ

354

355

356

357 **Results**

358 **PVL induces NETs efficiently in neutrophils from patients with recurrent**
359 **PVL-SA infections**

360 To determine why some individuals show increased susceptibility to recurrent PVL-
361 SA infections, we assessed neutrophil responses in these patients. To verify that
362 PVL induced cell death results in NETs [48,49], we stimulated control and patient
363 neutrophils with 1 nM PVL for 4 h and stained them with the DNA dye DAPI and
364 immuno-labeled with anti-NE and anti-chromatin antibodies (Figure 1A). As a
365 control we used PMA, a well characterized mitogen that induces NADPH-oxidase
366 dependent NETosis [60]. As shown by confocal microscopy, PVL and PMA induced
367 NET formation in both control and patient neutrophils. Interestingly, 0.1 nM PVL
368 killed neutrophils isolated from patients more efficiently than PMNs isolated from
369 healthy controls (Figure 1B) as measured with a cell impermeable DNA dye. Patient
370 and control neutrophils were equally susceptible to make NETs in response to PMA.

371 Given the binding specificity of PVL we checked the expression of CD45, CD88,
372 and C5L2, as well as the neutrophil activation markers CD63 and CD66b on control
373 and patient neutrophils by flow cytometry. Patient neutrophils expressed higher
374 levels of CD45 (adjusted p value = 0.000473), and there was no difference in
375 CD88. Furthermore, a subset of patients expressed increased C5L2 levels
376 compared to control neutrophils (Supplementary Figure S1A), but this trend was
377 not consistent for all patients (Figure 1C). Interestingly, the difference in
378 expression of C5L2 and possibly CD45 in patients compared to controls correlated
379 with the difference in NET formation in response to 0.1 nM PVL (ρ = 0.4491 for
380 CD45, ρ = 0.7105 for C5L2) (Figure 1D and 1E). Differences in expression levels
381 of CD88, CD63 or CD66b did not correlate with differences in NET formation
382 (Supplementary Figure S1B-D).

383 Neutrophils isolated from control and patient phagocytosed opsonized *Escherichia*
384 *coli* particles with equal efficiency; the proportion of neutrophils phagocytosing and
385 the average quantity of phagocytosed bacteria per cell were similar in both
386 neutrophil populations, suggesting normal phagocytic capacity of patient
387 neutrophils (Supplementary Figure S1E).

388 Taken together, our data show that neutrophils from patients with recurrent PVL-
389 SA infections express higher levels of the PVL receptor CD45 and make more NETs
390 in response to 0.1 nM PVL when compared to control neutrophils.

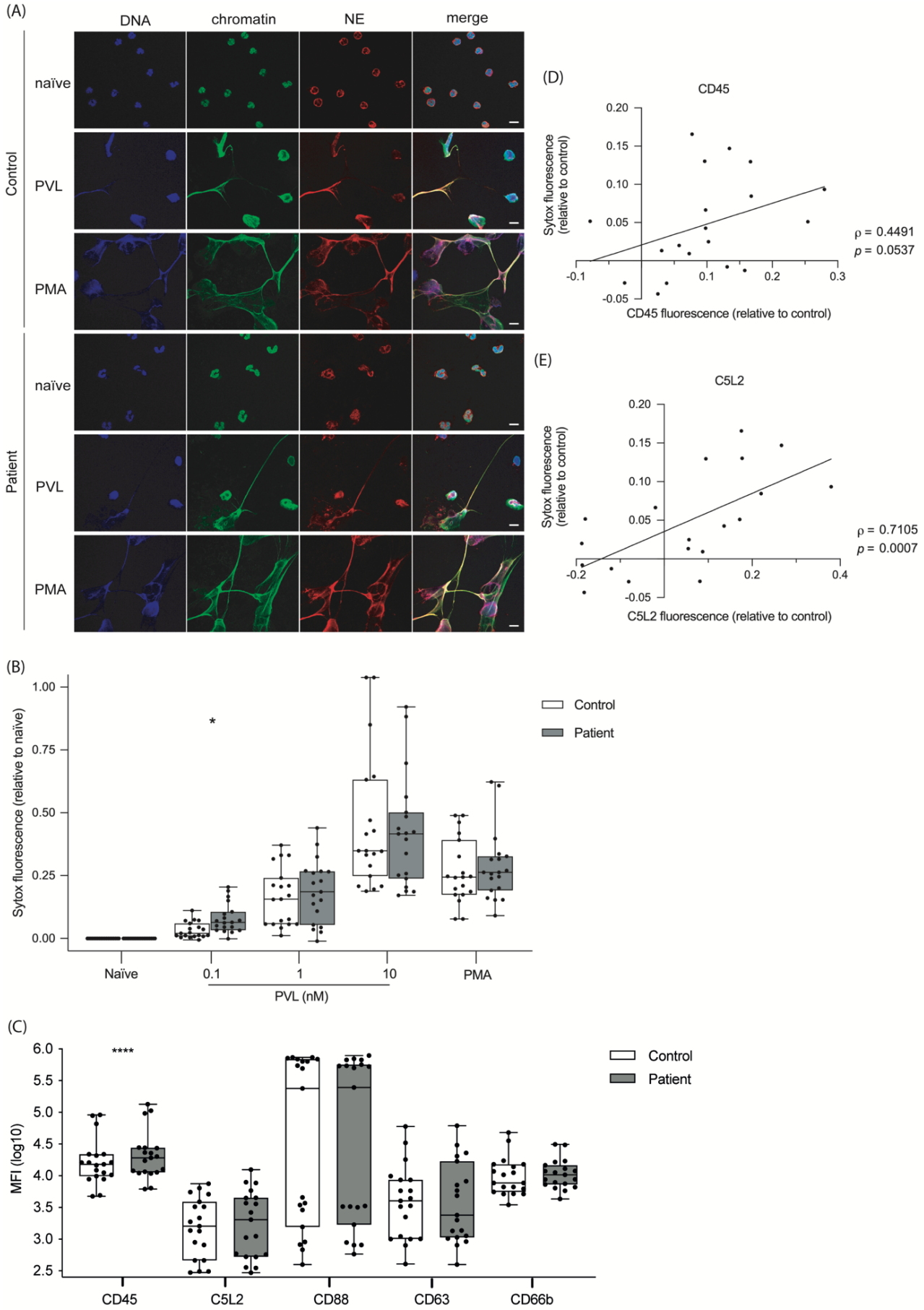

Figure 1. Neutrophils from patients with recurrent PVL-SA infections make more NETs in response to PVL and express more CD45 than neutrophils from healthy donors. (A) Representative confocal images of control and patient neutrophils, either naïve or stimulated with 50 nM PMA or 1 nM PVL, stained for DNA (blue), neutrophil elastase

427 (NE, red) and chromatin (green). Scale bar represents 10 µm. (B) Purified primary
428 neutrophils from patients suffering from recurrent PVL-SA infections (n=19) and healthy
429 controls (n=19) were either left untreated or stimulated with PMA (50 nM) or PVL (0.1 nM,
430 1 nM or 10 nM) for 4 h and cell death was quantified by adding the cell-impermeable DNA
431 dye SYTOX Green and measuring fluorescence. Boxplot indicates SYTOX fluorescence
432 relative to naïve neutrophils at 4 h. (C) CD45, C5L2, CD88, CD63 and CD66b were
433 immunolabelled on neutrophils from patients and healthy controls. The fluorescence was
434 measured and indicated as log-transformed MFI. (D) CD45 or (E) C5L2 fluorescence of
435 patient neutrophils relative to control was plotted against SYTOX fluorescence of patient
436 neutrophils relative to control after incubation with 0.1 nM PVL for 4 h. (B) Unpaired
437 Wilcoxon signed rank test with Bonferroni post-hoc test, * $P<0.05$. (C) Paired *t*-test, ***
438 $P<0.001$. (D-E) Spearman's correlation test where the coefficient of correlation (ρ) and
439 probability (p) are indicated. A best-fit line indicates the trend.

440

441 **PVL induces NETs independent from ROS**

442 NADPH-oxidase dependent superoxide formation is essential in NETs induced by
443 some stimuli [43], prompting us to investigate the NETosis pathway initiated by
444 PVL. We first tested superoxide generation in healthy primary neutrophils
445 stimulated with different concentrations of PVL or PMA. PVL stimulation resulted in
446 weak superoxide production at all concentrations (Figure 2A). In contrast, PMA
447 induced a significant superoxide burst.

448 We quantified ROS production as well as NET formation in neutrophils from CGD
449 patients. As expected, CGD neutrophils failed to generate superoxide in response
450 to PVL or PMA (Figure 2B). However, unlike PMA, PVL induced extracellular DNA
451 release (Figure 2C) and NET formation (Figure 2D and supplementary videos S1-
452 S8) in CGD neutrophils. These data show that while PVL stimulation weakly
453 activates NADPH-oxidase, NET formation is independent from the produced ROS.

454 Given the known involvement of various neutrophil proteins in NET formation, we
455 asked if PVL-induced NET formation could be blocked pharmacologically by the PKC
456 inhibitor Gö6983 (PKCi), the calcium chelator BAPTA-AM, the NADPH-oxidase
457 inhibitor DPI, the ROS scavenger pyrocatechol, the myeloperoxidase inhibitor
458 ABAH, the neutrophil elastase inhibitor NEi, or the pan serine protease inhibitor
459 AEBSF (Figure 2E-F and 2H). We observed that PKCi weakly inhibited NET
460 formation induced by 1 nM PVL (Figure 2E), whilst none of the other inhibitors,
461 including inhibitors of ROS-producing enzymes (DPI and ABAH) or ROS scavengers
462 (pyrocatechol), blocked NETosis induced by 1 or 10 nM PVL (Figure 2E-F and 2H).
463 Notably, neutrophils pre-treated with NEi or AEBSF and stimulated with 1nM PVL
464 formed smaller NETs (Figure 2H). These data suggest that PVL-mediated NET

465 formation is ROS- and protease-independent. As a control, we confirmed [43] that
466 PMA induced NET formation was blocked by all inhibitors tested (Figure 2G-H).

467 Mazzoleni *et al.* [49] suggested that small conductance calcium-activated
468 potassium (SK) channels and alternative ROS sources, such as mitochondria or
469 xanthine oxidase, mediate PVL-induced NETosis. To verify this, we pre-treated
470 neutrophils with the xanthine oxidase inhibitor allopurinol, the SK channel inhibitor
471 apamin, and the mitochondrial uncouplers DNP and FCCP, before stimulating with
472 either PMA or PVL. The SK channel inhibitor NS8593 was toxic to neutrophils in
473 our hands and was excluded from our experiments. At 1 nM, but not at 10 nM PVL
474 stimulation, allopurinol inhibited NET formation, whilst mitochondrial uncoupling
475 with FCCP partially inhibited NET formation. (Supplementary Figure S2A-B). These
476 findings were supported by confocal imaging (Supplementary Figure S2D). None
477 of the inhibitors affected PMA-induced NET formation (Supplementary Figure S2C).
478 Given that PVL induces NET formation in CGD patients despite a complete lack of
479 ROS (Figure 2B), and the inability of the ROS scavenger pyrocatechol to inhibit
480 PVL induced NETosis, the inhibition of NETs by allopurinol treatment or
481 mitochondrial uncoupling appears to be independent of ROS production. This is
482 further supported by the observation that DPI, which not only inhibits NADPH-
483 oxidase but all flavin-containing proteins including xanthine oxidase [61] and
484 mitochondrial complex I [62], did not block PVL induced NETosis (Figure 2E-F).
485 Finally, the inability of ROS-targeting inhibitors to block NETosis induced by 10 nM
486 PVL indicates that PVL-induced NETosis is independent from ROS production.

487

488

489

490

491

492

493

494

495

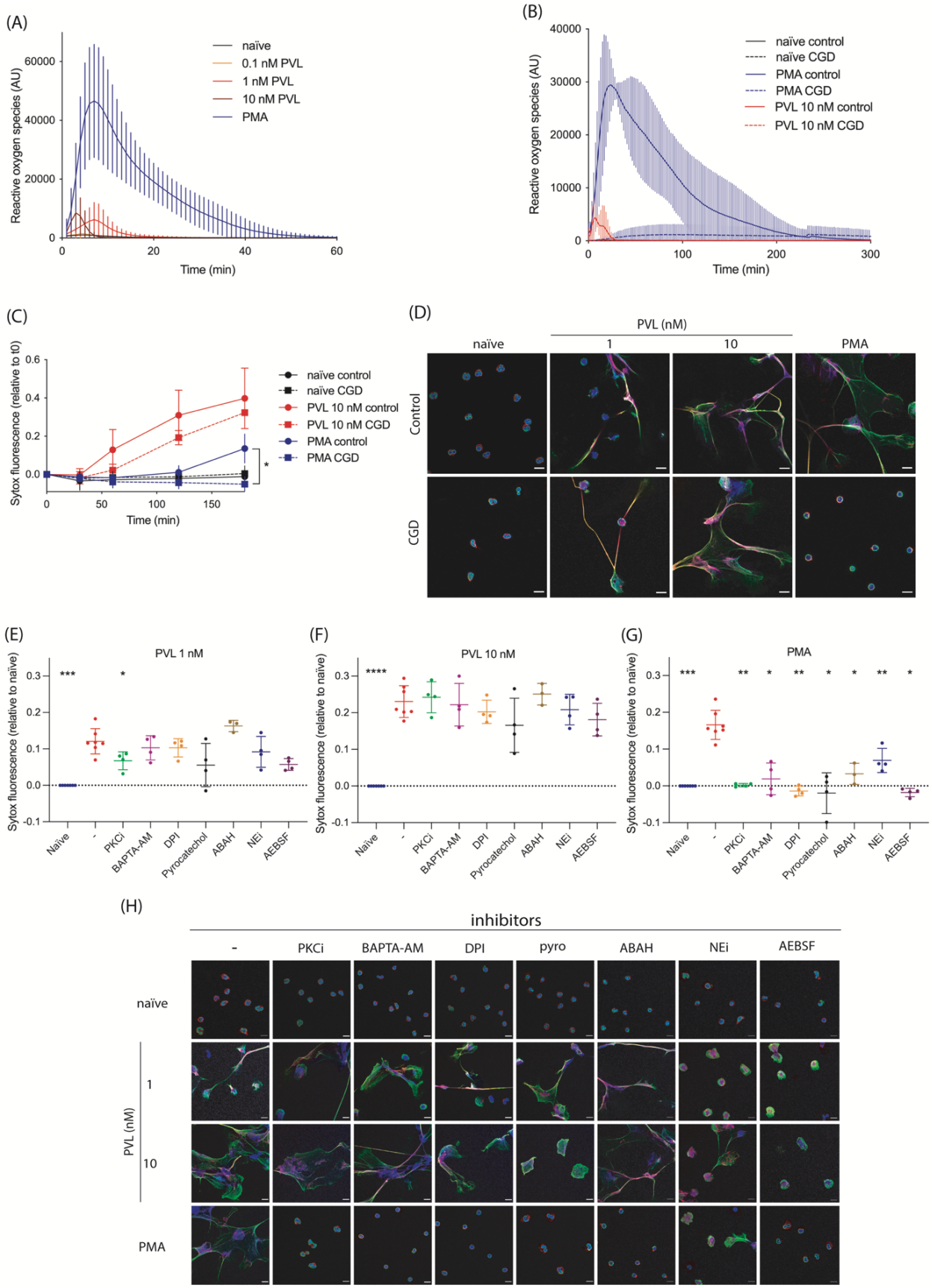

Figure 2. PVL induces ROS-independent NETosis. (A-B) Reactive oxygen species (ROS) formation was quantified in control (A n=14, B n=3) or CGD human primary neutrophils (n=3) stimulated with PMA (50 nM) or PVL (0.1 nM, 1 nM or 10 nM). (C) Control or CGD neutrophils (n=3) were stimulated with PMA (50 nM) or PVL (10 nM) for 3h and cell death was quantified using the cell impermeable DNA dye SYTOX Green. Indicated is SYTOX Green fluorescence relative to t = 0 min. (D) Representative confocal microscopy images of control and CGD patient neutrophils either naïve or stimulated with PMA (50 nM)

527 or PVL (1 nM or 10 nM) and stained for DNA (blue), NE (red) and chromatin (green). Scale
528 bar represents 10 µm. (E-G) Healthy human neutrophils were treated with PKC inhibitor
529 Gö6983 (PKCi, 1 µM), BAPTA-AM (10 µM), DPI (1 µM), pyrocatechol (30 µM), ABAH (500
530 µM), NEi (20 µM) and AEBSF (100 µM) for 30 min, before stimulating with (E) PVL 1 nM,
531 (F) PVL 10 nM or (G) PMA 50 nM for 4h. We quantified cell death with SYTOX Green and
532 the fluorescence signal relative to naïve is indicated. (H) Representative confocal
533 microscopy of naïve neutrophils or after stimulation with PMA or PVL (1 nM or 10 nM) in
534 the presence or absence of indicated inhibitors, and stained for DNA (blue), NE (red) and
535 chromatin (green). Scale bar represents 10 µm. (C) Two-way ANOVA with Tukey's post-
536 hoc test. *P<0.05. (E-G) Mean ±SD of four independent experiments. *P<0.05, **
537 P<0.01, *** P<0.001, one-way ANOVA with Dunnett´s multiple comparison test.

538

539 **PVL-induced NETs lack enrichment of key antimicrobial proteins**

540 Since PVL probably induces NETs through a non-canonical pathway we analyzed
541 the proteomes of NETs induced by PVL, PMA, and nigericin, an NADPH-oxidase
542 independent NET inducer [43]. We analyzed NETs from three independent donors
543 by quantitative mass spectrometry and compared them to the proteome of
544 unstimulated neutrophils. Principal component analysis revealed that PVL-, PMA-
545 and nigericin-induced NETs each have distinct proteomes (Figure 3A).
546 Interestingly, PVL NETs appear to cluster between naïve neutrophils and NETs
547 induced by PMA and nigericin, suggesting their proteome composition is
548 intermediate between naïve cells and classical NETs. Measurement of the Euclidean
549 distance between samples confirmed that PVL NETs are less distinct from naïve
550 neutrophils than are PMA- or nigericin-stimulated NETs (Supplementary Figure
551 S3A).

552 We detected 2458 distinct proteins in the combined NET samples (present in at
553 least two of three replicate experiments). To examine which proteins are driving
554 the differences between the NET proteomes, we performed a differential
555 enrichment analysis using a 2-fold change in protein abundance with an adjusted
556 p value below 0.01 as a cut-off. We found significant differences in relative protein
557 abundance between all three NET stimuli when compared with naïve neutrophils
558 (Figure 3B and Supplementary Figure S3A). Fewer differentially abundant proteins
559 (DAPs) were detected between PVL-induced NETs and naïve PMNs (194 significant)
560 compared to PMA- (449) and nigericin-induced NETs (670). These data suggest
561 that the specific enrichment or depletion of proteins during NETosis is lower or
562 incomplete in PVL-treated neutrophils.

563 Examination of the fold changes of NET-specific DAPs revealed that most DAPs
564 have the same pattern of enrichment or depletion across all types of NETs

565 compared to naïve neutrophils (459 with negative logFC, 294 positive logFC, Figure
566 3C). Regression of global DAP fold changes (Supplementary Figure S3B) revealed
567 that though most proteins have the same enrichment pattern across NETs, the
568 fold-changes are reduced in PVL- compared to PMA- and nigericin-induced NETs
569 (slopes = 0.64, and 0.49 respectively), while PMA and nigericin NETs have
570 equivalent DAP fold-changes (slope = 1).

571 K-means clustering of DAP fold change patterns supported this trend, and further
572 identified a cluster of proteins specifically enriched on nigericin induced NETs
573 (Figure 3C cluster two, orange, and Supplementary Table 2). To look more closely
574 at the differences between PVL-induced NETs and PMA- or nigericin-induced NETs,
575 we performed pair-wise comparisons between PVL and PMA or PVL and nigericin
576 (Supplementary Figure S3C and S3D) and ranked the 25 most abundant DAPs
577 (Figure 3D and 3E, respectively). Among these, key neutrophil proteins NE
578 (ELANE), PRTN3, and CAMP, were all less abundant on PVL-induced NETs
579 compared with PMA- or nigericin-induced NETs. In contrast, we found cytoskeleton
580 proteins such as actin (ACTB), myosin (MYH9), and tubulin (TUBA1B) to be more
581 enriched on PVL NETs. Our data suggest that PVL induces NETs with a different
582 NET proteome assembly when compared with PMA or nigericin, resulting in a lack
583 of enrichment of key antimicrobial proteins on PVL NETs.

584

585

586

587

588

589

590

591

592

593

594

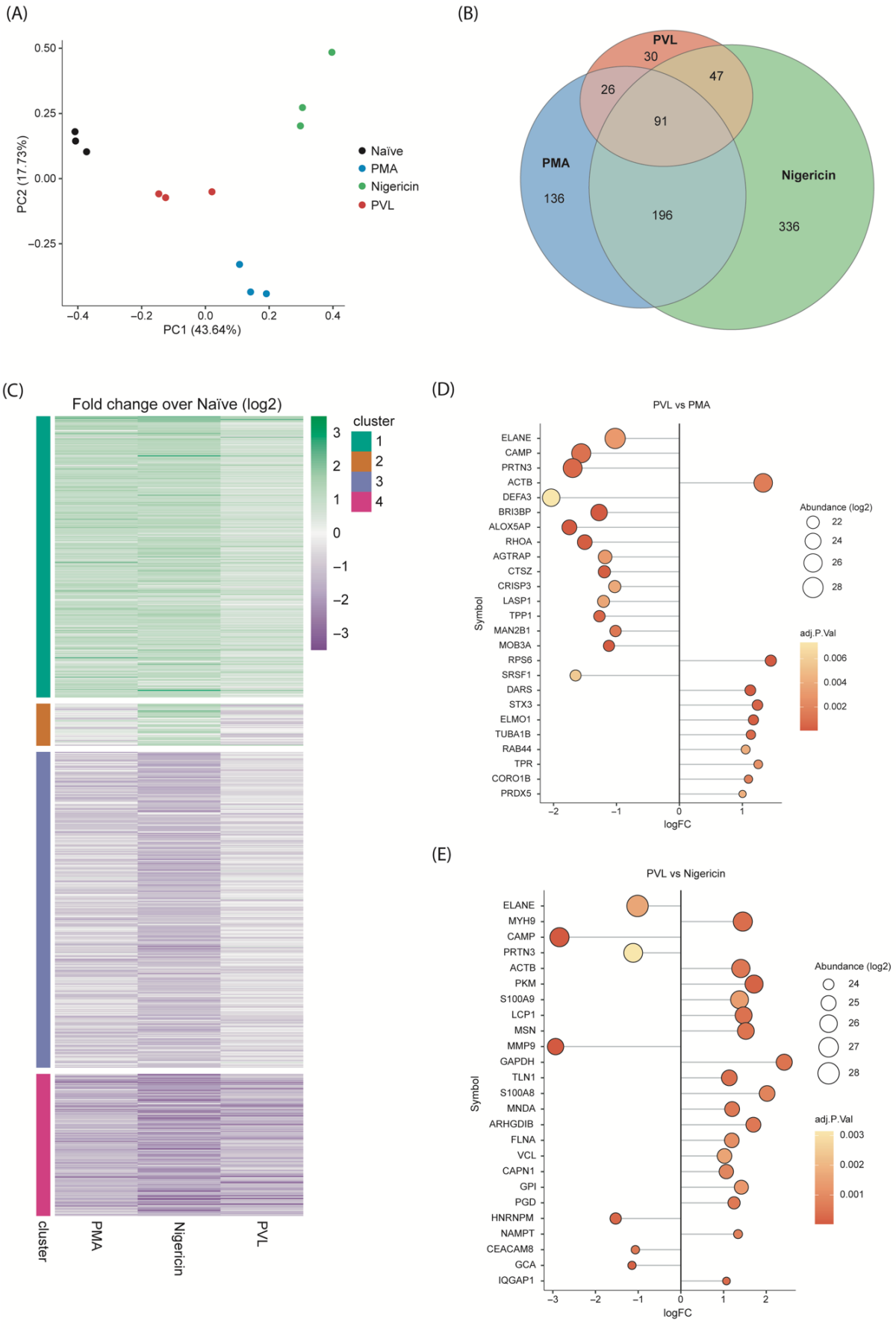

Figure 3. NET proteome assembly is different in PVL-induced NETs. (A) Principal component analysis of the proteomes of naïve neutrophils, and PVL-, PMA-, and nigericin-induced NETs. Analysis was performed on scaled log2-abundance of all proteins detected in at least 2/3 replicates. (B) Euler diagram showing the number and distribution of significant Differentially Abundant Peptides (logFC > 1, adjusted p < 0.01) on NETs

compared to naïve neutrophils. Areas are proportional to DAP set size. (C) Clustered heatmap showing fold change (log2) values on each NET sample compared to naïve neutrophils of significant DAPs from (B). Clustering was performed by k-means algorithm with k=4 clusters. (D-E) Top 25 most-abundant DAPs that are significantly differentially abundant on PVL-induced NETs compared with PMA- (D) and nigericin-induced NETs (E). Point size and fill color represent average abundance across samples and adjusted *p* value, respectively. Proteomes were made from n=3 samples per condition from independent donors. DAP significance for each comparison was determined by a threshold of |[log2 fold change]| > 1 and adjusted *p* value < 0.01.

PVL-induced NETs are less bactericidal

Given the differential enrichment of antimicrobial proteins in PMA- compared to PVL induced NETs, we hypothesized that their bactericidal activity is different. We incubated methicillin-resistant *S. aureus* (MRSA) with either PMA- or PVL induced NETs for 1 h, harvested the bacteria, and quantified the surviving colony forming units. PVL-induced NETs did not kill *S. aureus*, whilst PMA-induced NETs did (Figure 4A). We verified that both stimuli at these concentrations released similar amounts of NETs by nanodrop DNA quantification (Figure 4B). These results show that PVL NETs have a lower antimicrobial potential against MRSA than PMA NETs.

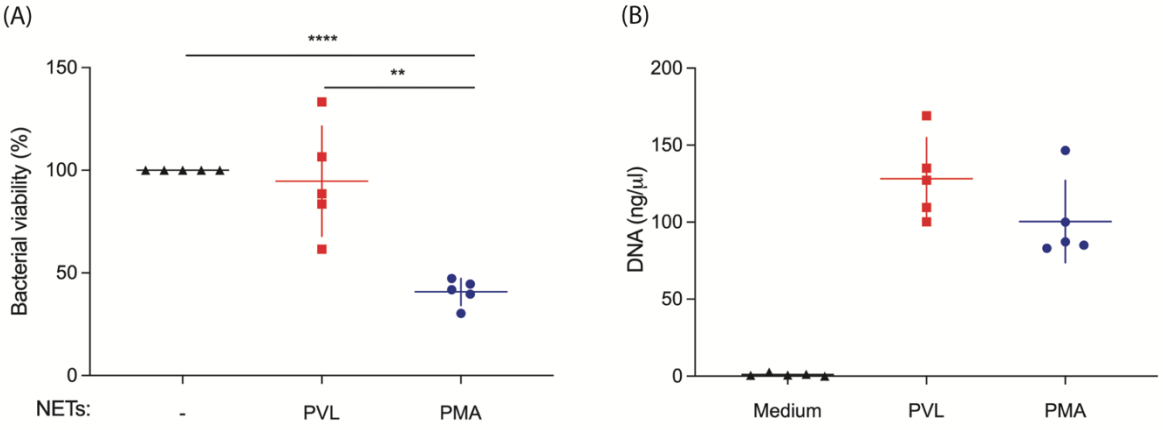

Figure 4. PVL-induced NETs do not kill MRSA. (A) Primary human neutrophils were stimulated with PMA (200 nM) or PVL (100 nM) for 3 h to induce NETs. MRSA was incubated with NETs for 1 h and CFU was quantified. Bacterial viability is expressed as a percentage of CFUs normalized to MRSA incubated in the absence of NETs. (B) The DNA content of PMA and PVL induced NETs at 3 h was quantified by spectrophotometry. (A) mean ± SD of five or four independent experiments. **p<0.01, **** p<0.0001, two-tailed paired *t* test.

656 **Discussion**

657 The reporting of PVL-SA infections has increased in the past few decades.
658 Interestingly, human host factors that mediate susceptibility or severity of PVL-SA
659 infections are not known. To identify these factors, we determined functional
660 responses of neutrophils, a major cellular target of PVL, in response to PVL in
661 patients that suffer from recurrent PVL-SA infections. We identified increased NET
662 formation in patient neutrophils upon stimulation with a low PVL concentration.
663 (Figure 1B), and a higher expression of CD45 and potentially C5L2, two of the
664 toxin's receptors (Figure 1C), in patient neutrophils compared to healthy controls.
665 Furthermore, the increase in CD45 and C5L2 expression correlated with more NET
666 formation induced by PVL (Figure 1D-E).

667 LukS-PV and LukF-PV have different binding affinities to their respective receptors
668 (C5L2 and CD88 for LukS-PV, CD45 for LukF-PV), and the low binding affinity of
669 LukF-PV to CD45 suggests that varying expression levels of CD45 are unlikely to
670 modulate pore formation [35]. In contrast, LukS-PV binding affinity to C5aR or
671 C5L2 is much higher and therefore their expression may modulate sensitivity to
672 PVL toxin. Given that neutrophils express C5L2 less abundantly than C5aR, it was
673 surprising to find that differential expression of C5L2 correlates with an increased
674 sensitivity of patient neutrophils to PVL (Figure 1E) [36]. However, the binding
675 affinities of LukS-PV to C5aR and C5L2 and the relative contribution of C5L2 to PVL
676 mediated cell death is not known. Whether there is a genetic predisposition in
677 patients with recurrent PVL-SA remains to be determined and we are currently
678 investigating avenues to study this.

679 C5aR localizes to the plasma membrane, rendering it accessible for extracellular
680 PVL toxin. However, there are conflicting reports on the localization of C5L2 since
681 it has been detected both intracellularly and on the plasma membrane [63,64].
682 We detected C5L2 on the plasma membrane through flow cytometry (Figure 1C),
683 suggesting that the expression is not exclusively intracellular. However, much is
684 unknown concerning the regulation of C5L2 and C5aR expression and receptor
685 shuttling and it is unclear how this regulation might affect targeting by PVL
686 [63,64].

687 Pore formation by PVL is described to exert various cellular effects, intracellular
688 calcium flux, ATP-release into the extracellular environment, induction of apoptosis
689 and cellular lysis [65]. These various phenotypes likely depend on the toxin

690 concentration a cell encounters. We therefore characterized NETosis at different
691 PVL concentrations.

692 NET formation induced by PMA or *Candida albicans* is ROS-dependent and is
693 blocked by compounds that scavenge ROS or inhibit ROS [43]. Other stimuli, like
694 nigericin and calcium ionophores induce NETs through a ROS independent
695 mechanism [43]. PVL induces the formation of NETs independently of NADPH-
696 oxidase and MPO activity, two enzymes that produce ROS. This is evidenced by
697 two observations (1) CGD neutrophils do not produce ROS upon stimulation with
698 PVL (Figure 2B), but make NETs (Figure 2C-D) and (2) DPI, an inhibitor of flavin-
699 containing proteins such as NADPH-oxidase, xanthine oxidase [61], and
700 cytochrome C [62,66], the ROS scavenger pyrocatechol, and the MPO inhibitor
701 ABAH all fail to inhibit PVL-induced NET formation (Figure 2E-H).

702 A recent study by Mazzoleni *et al*. suggested that ROS derived from mitochondria
703 or xanthine oxidase are involved in PVL-induced NETosis [49]. We observed that
704 mitochondrial uncoupling by DNP or FCCP as well as xanthine oxidase inhibition by
705 allopurinol partly inhibited PVL-induced NET formation (Supplementary Figure 2A-
706 C). Xanthine oxidoreductase consists of two isoforms, xanthine oxidase and
707 xanthine dehydrogenase. Allopurinol inhibits both isoforms, which affects purine
708 metabolism. Moreover, allopurinol itself generates superoxide radicals upon
709 inhibition of xanthine oxidase [67]. Therefore its inhibitory effect on PVL-induced
710 NET formation may be independent from xanthine oxidase inhibition or ROS
711 formation. How allopurinol exerts its inhibitory effects on PVL-induced NET
712 formation is still unclear. Furthermore, given that both DPI and the ROS scavenger
713 pyrocatechol were unable to inhibit PVL-induced NET formation (Figure 2E-H), we
714 hypothesize that the inhibitory effect of allopurinol and FCCP is independent from
715 their effects on ROS production. Notably, inhibition of NET formation by these
716 inhibitors was seen at 1 nM PVL, but was lost when stimulating with 10 nM PVL. It
717 may be that PVL at high concentrations is able to induce NET formation without
718 the involvement of neutrophil components interrogated by the inhibitors used in
719 our study, whilst at low PVL concentrations some components may contribute to
720 NET formation.

721 Neutrophil proteases were not essential for PVL-induced NET formation, although
722 we did observe that formed NETs appeared smaller upon protease inhibition
723 (Figure 2H). Neutrophil elastase is known to contribute to chromatin

724 decondensation during NADPH-oxidase dependent NETosis [44,68] and this
725 decondensation may occur during PVL-mediated NET formation as well
726 (Supplementary Videos S3-4).

727 Interestingly, different NETosis mechanisms lead to NETs with specific
728 compositions. We find differences in protein abundances of NETs induced by PVL,
729 PMA, or nigericin, and that specifically PVL NETs appear to be less distinct from
730 unstimulated neutrophils (Figure 3A). Several antimicrobial proteins are less
731 abundant in PVL-induced NETs, when compared to PMA- or nigericin-induced NETs
732 (Figure 3D-E). In contrast, cytoskeletal proteins are more abundant on PVL NETs.
733 A previous report also identified a similar enrichment of cytoskeletal proteins in
734 spontaneously lysed neutrophils [69]. Given PMA or nigericin-induced NET
735 formation involves an intracellular release of granular components [68], this
736 'mixing-of-the-bag' may allow for efficient tethering of granular components to the
737 chromatin backbone and degradation of the cytoskeleton. Cell lysis occurs 2-3 h
738 after stimulation with PMA (Figure 2C and Supplementary Videos S1-S8), while
739 PVL-induced NET formation occurs swiftly, with cell lysis occurring within the first
740 2 h after stimulation. We speculate that granular components may be lost to the
741 extracellular environment during this rapid lysis, resulting in a less bactericidal
742 NET (Figure 4A). These data suggest that NETs induced by different stimuli may
743 display different functional characteristics. Leukocidins such as PVL may have
744 evolved to elicit a harmless form of NET formation to promote survival of the
745 invading bacteria.

746 NETs have at least three described functions, they are antimicrobial [42],
747 procoagulant [70], and activate the immune system [71,72]. PVL-SA infections
748 may be associated with a higher risk for thrombotic events. In addition to being
749 less antimicrobial, it would be interesting to investigate if PVL-induced NETs also
750 differ in their procoagulant or immune activation functions.

751 In conclusion, our observation of (a) differentially expressed PVL receptors in
752 individuals with recurrent or severe PVL-SA infections and (b) functionally different
753 NET formation after neutrophil exposure to PVL in contrast to other stimuli may
754 explain specific clinical features and interindividual differences in PVL-SA
755 infections. We propose that overexpression of PVL receptors makes a PVL-SA
756 infected patient more prone to this disarmed NET formation, preventing efficient
757 clearance of the invading bacteria. In turn, this could provide a competitive

758 advantage to PVL-SA, facilitating colonization and recurrent infections. Further
759 investigations are necessary to verify this finding and find potential treatment or
760 prevention strategies for these infections.

761

762 **Acknowledgements**

763 We thank Christian Frese from the Proteomics Research Platform at the Max Planck
764 Unit for the Science of Pathogens for proteomic analysis.

765 We thank Alf Herzig for visualizing PVL-induced NET formation in healthy and CGD
766 neutrophils in real time by confocal microscopy.

767

768 **Author Contributions**

769 HJ, AZ, RK, and GM designed the study

770 HJ, DC, and GM performed experiments and analyzed the data

771 HVB and RK cared for the patients

772 AL, LGH, RL, JTS, MSS, MS, and HVB have interpreted the data and revised the
773 manuscript for important intellectual content

774 CJH analyzed the mass spectrometry data

775 HJ, AZ, RK, and GM wrote the manuscript

776

777 **Competing interests**

778 The authors declare that they have no competing interests.

779

780

781

782

783

784

785 **References**

786 1. Bogaert D, van Belkum A, Sluijter M, Luijendijk A, de Groot R, Rümke H, et
787 al. Colonisation by Streptococcus pneumoniae and Staphylococcus aureus
788 in healthy children. Lancet. 2004;363: 1871–1872. doi:10.1016/S0140-
789 6736(04)16357-5

790 2. Wertheim HFL, Melles DC, Vos MC, van Leeuwen W, van Belkum A,
791 Verbrugh HA, et al. The role of nasal carriage in Staphylococcus aureus
792 infections. Lancet Infect Dis. 2005;5: 751–62. doi:10.1016/S1473-
793 3099(05)70295-4

794 3. Tromp AT, van Strijp JAG. Studying Staphylococcal Leukocidins: A
795 Challenging Endeavor. Front Microbiol. 2020;11: 1–8.
796 doi:10.3389/fmicb.2020.00611

797 4. Müller-Premru M, Strommenger B, Alikadic N, Witte W, Friedrich AW, Seme
798 K, et al. New strains of community-acquired methicillin-resistant
799 Staphylococcus aureus with Panton-Valentine leukocidin causing an
800 outbreak of severe soft tissue infection in a football team. Eur J Clin
801 Microbiol Infect Dis. 2005;24. doi:10.1007/s10096-005-0048-0

802 5. Gilbert M, MacDonald J, Louie M, Gregson D, Zhang K, Elsayed S, et al.
803 Prevalence of USA300 colonization or infection and associated variables
804 during an outbreak of community-associated methicillin-resistant
805 Staphylococcus aureus in a marginalized urban population. Can J Infect Dis
806 Med Microbiol. 2007;18. doi:10.1155/2007/597123

807 6. Carré N, Sillam F, Dabas JP, Herbreteau N, Pinchon C, Ortmans C, et al.
808 Staphylococcus aureus carrying Panton-Valentine leukocidin genes nasal
809 colonization and skin infection: Screening in case of outbreak in a school
810 environment. Med Mal Infect. 2008;38.
811 doi:10.1016/j.medmal.2008.06.025

812 7. Carré N, Herbreteau N, Askeur N, Dabas JP, Pinchon C, Bes M, et al.
813 Outbreak of skin infections due to Staphylococcus aureus carrying Panton-
814 Valentine leukocidin genes in pupils and their relatives. Med Mal Infect.
815 2011;41. doi:10.1016/j.medmal.2010.12.017

816 8. Higashiyama M, Ito T, Han X, Nishiyama J, Tanno A, Wada T, et al. Trial to

817 control an outbreak of Panton-Valentine leukocidin-positive methicillin-
818 resistant Staphylococcus aureus at a boarding school in Japan. Am J Infect
819 Control. 2011;39. doi:10.1016/j.ajic.2011.02.010

820 9. Bourigault C, Corvec S, Brulet V, Robert P-Y, Mounoury O, Goubin C, et al.
821 Outbreak of Skin Infections Due to Panton-Valentine Leukocidin-Positive
822 Methicillin-Susceptible Staphylococcus aureus in a French Prison in 2010-
823 2011. PLoS Curr. 2014.
824 doi:10.1371/currents.outbreaks.e4df88f057fc49e2560a235e0f8f9fea

825 10. Couvé-Deacon E, Tristan A, Pestourie N, Faure C, Doffoel-Hantz V, Garnier
826 F, et al. Outbreak of Panton-valentine leukocidin–associated methicillin-
827 susceptible staphylococcus aureus infection in a rugby team, France, 2010–
828 2011. Emerg Infect Dis. 2016;22. doi:10.3201/eid2201.150597

829 11. Leistner R, Kola A, Gastmeier P, Krüger R, Hoppe P-A, Schneider-Burrus S,
830 et al. Pyoderma outbreak among kindergarten families: Association with a
831 Panton-Valentine leukocidin (PVL)-producing S. aureus strain. Becker K,
832 editor. PLoS One. 2017;12: e0189961. doi:10.1371/journal.pone.0189961

833 12. Ismail H, Govender NP, Singh-Moodley A, Van Schalkwyk E, Shuping L,
834 Moema I, et al. An outbreak of cutaneous abscesses caused by Panton-
835 Valentine leukocidin-producing methicillin-susceptible Staphylococcus
836 aureus among gold mine workers, South Africa, November 2017 to March
837 2018. BMC Infect Dis. 2020;20. doi:10.1186/s12879-020-05352-5

838 13. Linde H, Wagenlehner F, Strommenger B, Drubel I, Tanzer J, Reischl U, et
839 al. Healthcare-associated outbreaks and community-acquired infections due
840 to MRSA carrying the Panton-Valentine leucocidin gene in southeastern
841 Germany. Eur J Clin Microbiol Infect Dis. 2005;24. doi:10.1007/s10096-
842 005-1341-7

843 14. Wagenlehner FME, Naber KG, Bambl E, Raab U, Wagenlehner C, Kahlau D,
844 et al. Management of a large healthcare-associated outbreak of Panton-
845 Valentine leucocidin-positive meticillin-resistant Staphylococcus aureus in
846 Germany. J Hosp Infect. 2007;67. doi:10.1016/j.jhin.2007.07.006

847 15. Tang CT, Nguyen DT, Hoa NT, Nguyen TMP, Le VT, To SD, et al. An
848 outbreak of severe infections with community-acquired MRSA carrying the
849 panton-valentine leukocidin following vaccination. PLoS One. 2007;2.

850 doi:10.1371/journal.pone.0000822

851 16. Maltezou HC, Vourli S, Katerelos P, Maragos A, Kotsalidou S, Remoudaki E,
852 et al. Panton-Valentine leukocidin-positive methicillin-resistant
853 Staphylococcus aureus outbreak among healthcare workers in a long-term
854 care facility. Int J Infect Dis. 2009;13. doi:10.1016/j.ijid.2009.02.004

855 17. Teare L, Shelley OP, Millership S, Kearns A. Outbreak of Panton-Valentine
856 leucocidin-positive meticillin-resistant Staphylococcus aureus in a regional
857 burns unit. J Hosp Infect. 2010;76. doi:10.1016/j.jhin.2010.04.023

858 18. Nagao M, Iinuma Y, Suzuki M, Matsushima A, Takakura S, Ito Y, et al. First
859 outbreak of methicillin-resistant Staphylococcus aureus USA300 harboring
860 the Panton-Valentine leukocidin genes among Japanese health care
861 workers and hospitalized patients. Am J Infect Control. 2010;38.
862 doi:10.1016/j.ajic.2010.04.214

863 19. Ali H, Nash JQ, Kearns AM, Pichon B, Vasu V, Nixon Z, et al. Outbreak of a
864 South West Pacific clone Panton-Valentine leucocidin-positive meticillin-
865 resistant Staphylococcus aureus infection in a UK neonatal intensive care
866 unit. J Hosp Infect. 2012;80. doi:10.1016/j.jhin.2011.12.019

867 20. Pinto AN, Seth R, Zhou F, Tallon J, Dempsey K, Tracy M, et al. Emergence
868 and control of an outbreak of infections due to Panton-Valentine leukocidin
869 positive, ST22 methicillin-resistant Staphylococcus aureus in a neonatal
870 intensive care unit. Clin Microbiol Infect. 2013;19. doi:10.1111/j.1469-
871 0691.2012.03987.x

872 21. Garvey MI, Bradley CW, Holden KL, Oppenheim B. Outbreak of clonal
873 complex 22 Panton–Valentine leucocidin-positive methicillin-resistant
874 Staphylococcus aureus. J Infect Prev. 2017;18.
875 doi:10.1177/1757177417695647

876 22. Kossow A, Kampmeier S, Schaumburg F, Knaack D, Moellers M, Mellmann
877 A. Whole genome sequencing reveals a prolonged and spatially spread
878 nosocomial outbreak of Panton–Valentine leucocidin-positive meticillin-
879 resistant Staphylococcus aureus (USA300). J Hosp Infect. 2019;101.
880 doi:10.1016/j.jhin.2018.09.007

881 23. Panigrahy A, Sinha S, Das BK, Kapil A, Vishnubhatla S, Dhawan B.

882 Staphylococcus aureus Colonisation in HIV-Infected Patients: Incidence,
883 Risk Factors and Subsequent Skin- and Soft-Tissue Infections. Indian J Med
884 Microbiol. 2020;38: 444–447. doi:10.4103/ijmm.IJMM_20_5

885 24. Ikeuchi K, Adachi E, Sasaki T, Suzuki M, Lim LA, Saito M, et al. An
886 Outbreak of USA300 Methicillin-Resistant Staphylococcus aureus Among
887 People With HIV in Japan. J Infect Dis. 2021;223: 610–620.
888 doi:10.1093/infdis/jiaa651

889 25. Shallcross LJ, Fragaszy E, Johnson AM, Hayward AC. The role of the
890 Panton-Valentine leucocidin toxin in staphylococcal disease: A systematic
891 review and meta-analysis. Lancet Infect Dis. 2013;13. doi:10.1016/S1473-
892 3099(12)70238-4

893 26. Saeed K, Gould I, Espositio S, Ahmad-Saeed N, Ahmed SS, Alp E, et al.
894 Panton–Valentine leukocidin-positive Staphylococcus aureus: a position
895 statement from the International Society of Chemotherapy. Int J
896 Antimicrob Agents. 2018;51: 16–25.
897 doi:10.1016/j.ijantimicag.2017.11.002

898 27. Hoppe P-A, Holzhauer S, Lala B, Bührer C, Gratopp A, Hanitsch LG, et al.
899 Severe infections of Panton-Valentine leukocidin positive Staphylococcus
900 aureus in children. Medicine (Baltimore). 2019;98: e17185.
901 doi:10.1097/MD.0000000000017185

902 28. Rimoldi SG, Pileri P, Mazzocco MI, Romeri F, Bestetti G, Calvagna N, et al.
903 The Role of Staphylococcus aureus in Mastitis: A Multidisciplinary Working
904 Group Experience. J Hum Lact. 2020;36. doi:10.1177/0890334419876272

905 29. Le Thomas I, Mariani-Kurkdjian P, Collignon A, Gravet A, Clermont O,
906 Brahimi N, et al. Breast milk transmission of a Panton-Valentine leukocidin-
907 producing Staphylococcus aureus strain causing infantile pneumonia. J Clin
908 Microbiol. 2001;39. doi:10.1128/JCM.39.2.728-729.2001

909 30. Labandeira-Rey M, Couzon F, Boisset S, Brown EL, Bes M, Benito Y, et al.
910 Staphylococcus aureus Panton-Valentine leukocidin causes necrotizing
911 pneumonia. Science (80-). 2007;315. doi:10.1126/science.1137165

912 31. Gillet Y, Issartel B, Vanhems P, Lina G, Vandenesch F, Etienne J, et al.
913 Severe staphylococcal pneumonia in children. Arch Pédiatrie. 2001;8.

914 doi:10.1016/S0929-693X(01)80190-1

915 32. Li HT, Zhang TT, Huang J, Zhou YQ, Zhu JX, Wu BQ. Factors associated
916 with the outcome of life-threatening necrotizing pneumonia due to
917 community-acquired Staphylococcus aureus in adult and adolescent
918 patients. Respiration. 2011;81. doi:10.1159/000319557

919 33. Duployez C, Le Guern R, Tinez C, Lejeune AL, Robriquet L, Six S, et al.
920 Panton-valentine leukocidin secreting staphylococcus aureus pneumonia
921 complicating COVID-19. Emerg Infect Dis. 2020;26: 1939–1941.
922 doi:10.3201/eid2608.201413

923 34. Schaumburg F, Witten A, Flamen A, Stoll M, Alabi AS, Kremsner PG, et al.
924 Complement 5a Receptor Polymorphisms Are Associated With Panton-
925 Valentine Leukocidin–positive Staphylococcus aureus Colonization in African
926 Pygmies. Clin Infect Dis. 2018; 1–3. doi:10.1093/cid/ciy666

927 35. Tromp AT, Van Gent M, Abrial P, Martin A, Jansen JP, De Haas CJC, et al.
928 Human CD45 is an f-component-specific receptor for the staphylococcal
929 toxin Panton-Valentine leukocidin. Nat Microbiol. 2018;3: 708–717.
930 doi:10.1038/s41564-018-0159-x

931 36. Spaan AN, Henry T, Van Rooijen WJM, Perret M, Badiou C, Aerts PC, et al.
932 The staphylococcal toxin panton-valentine leukocidin targets human C5a
933 receptors. Cell Host Microbe. 2013;13: 584–594.
934 doi:10.1016/j.chom.2013.04.006

935 37. Alonzo F, Torres VJ. Bacterial Survival Amidst an Immune Onslaught: The
936 Contribution of the Staphylococcus aureus Leukotoxins. PLoS Pathog.
937 2013;9: e1003143. doi:10.1371/journal.ppat.1003143

938 38. Spaan AN, Van Strijp JAG, Torres VJ. Leukocidins: Staphylococcal bi-
939 component pore-forming toxins find their receptors. Nature Reviews
940 Microbiology. Nature Publishing Group; 2017. pp. 435–447.
941 doi:10.1038/nrmicro.2017.27

942 39. Holzinger D, Gieldon L, Mysore V, Nippe N, Taxman DJ, Duncan JA, et al.
943 Staphylococcus aureus Panton-Valentine leukocidin induces an
944 inflammatory response in human phagocytes via the NLRP3 inflammasome.
945 J Leukoc Biol. 2012;92: 1069–1081. doi:10.1189/jlb.0112014

946 40. van Kessel KPM, Bestebroer J, van Strijp JAG. Neutrophil-Mediated
947 Phagocytosis of Staphylococcus aureus. Front Immunol. 2014;5: 467.
948 doi:10.3389/fimmu.2014.00467

949 41. Buvelot H, Posfay-Barbe KM, Linder P, Schrenzel J, Krause KH.
950 Staphylococcus aureus, phagocyte NADPH oxidase and chronic
951 granulomatous disease. FEMS Microbiol Rev. 2017;41.
952 doi:10.1093/femsre/fuw042

953 42. Brinkmann V, Reichard U, Goosmann C, Fauler B, Uhlemann Y, Weiss DS,
954 et al. Neutrophil extracellular traps kill bacteria. Science. 2004;303: 1532–
955 5. doi:10.1126/science.1092385

956 43. Kenny EF, Herzig A, Krüger R, Muth A, Mondal S, Thompson PR, et al.
957 Diverse stimuli engage different neutrophil extracellular trap pathways.
958 Elife. 2017;6: e24437. doi:10.7554/eLife.24437

959 44. Papayannopoulos V, Metzler KD, Hakkim A, Zychlinsky A. Neutrophil
960 elastase and myeloperoxidase regulate the formation of neutrophil
961 extracellular traps. J Cell Biol. 2010;191: 677–691.
962 doi:10.1083/jcb.201006052

963 45. Fuchs TA, Abed U, Goosmann C, Hurwitz R, Schulze I, Wahn V, et al. Novel
964 cell death program leads to neutrophil extracellular traps. J Cell Biol.
965 2007;176: 231–241. doi:10.1083/jcb.200606027

966 46. Sollberger G, Choidas A, Burn GL, Habenberger P, Di Lucrezia R, Kordes S,
967 et al. Gasdermin D plays a vital role in the generation of neutrophil
968 extracellular traps. Sci Immunol. 2018;3: eaar6689.
969 doi:10.1126/sciimmunol.aar6689

970 47. Pilsczek FH, Salina D, Poon KKH, Fahey C, Yipp BG, Sibley CD, et al. A
971 Novel Mechanism of Rapid Nuclear Neutrophil Extracellular Trap Formation
972 in Response to Staphylococcus aureus. J Immunol. 2010;185: 7413–7425.
973 doi:10.4049/jimmunol.1000675

974 48. Bhattacharya M, Berends ETM, Chan R, Schwab E, Roy S, Sen CK, et al.
975 Staphylococcus aureus biofilms release leukocidins to elicit extracellular
976 trap formation and evade neutrophil-mediated killing. Proc Natl Acad Sci U
977 S A. 2018;115: 7416–7421. doi:10.1073/pnas.1721949115

978 49. Mazzoleni V, Zimmermann-Meisse G, Smirnova A, Tarassov I, Prévost G.
979 Staphylococcus aureus Panton-Valentine Leukocidin triggers an alternative
980 NETosis process targeting mitochondria. FASEB J. 2020; 1–22.
981 doi:10.1096/fj.201902981R

982 50. Berends ETM, Horswill AR, Haste NM, Monestier M, Nizet V, Von Köckritz-
983 Blickwede M. Nuclease expression by Staphylococcus aureus facilitates
984 escape from neutrophil extracellular traps. J Innate Immun. 2010;2: 576–
985 586. doi:10.1159/000319909

986 51. Heyworth PG, Cross AR, Curnutte JT. Chronic granulomatous disease. Curr
987 Opin Immunol. 2003;15: 578–84. doi:10.1016/s0952-7915(03)00109-2

988 52. Hughes CS, Moggridge S, Müller T, Sorensen PH, Morin GB, Krijgsveld J.
989 Single-pot, solid-phase-enhanced sample preparation for proteomics
990 experiments. Nat Protoc. 2019;14: 68–85. doi:10.1038/s41596-018-0082-
991 x

992 53. Plubell DL, Wilmarth PA, Zhao Y, Fenton AM, Minnier J, Reddy AP, et al.
993 Extended Multiplexing of Tandem Mass Tags (TMT) Labeling Reveals Age
994 and High Fat Diet Specific Proteome Changes in Mouse Epididymal Adipose
995 Tissue. Mol Cell Proteomics. 2017;16: 873–890.
996 doi:10.1074/mcp.M116.065524

997 54. Robinson MD, McCarthy DJ, Smyth GK. edgeR: a Bioconductor package for
998 differential expression analysis of digital gene expression data.
999 Bioinformatics. 2010;26: 139–140. doi:10.1093/BIOINFORMATICS/BTP616

1000 55. Ritchie ME, Phipson B, Wu D, Hu Y, Law CW, Shi W, et al. limma powers
1001 differential expression analyses for RNA-sequencing and microarray
1002 studies. Nucleic Acids Res. 2015;43: e47–e47. doi:10.1093/nar/gkv007

1003 56. Kammers K, Cole RN, Tiengwe C, Ruczinski I. Detecting Significant
1004 Changes in Protein Abundance. EuPA open proteomics. 2015;7: 11–19.
1005 doi:10.1016/j.euprot.2015.02.002

1006 57. Larsson J. eulerr: Area-Proportional Euler and Venn Diagrams with Ellipses.
1007 R package version 6.1.1. 2021. Available: https://cran.r-
1008 project.org/package=eulerr

1009 58. Kolde R. pheatmap: Pretty Heatmaps. R package version 1.0.12. 2019.

1010 59. Perez-Riverol Y, Csordas A, Bai J, Bernal-Llinares M, Hewapathirana S,
1011 Kundu DJ, et al. The PRIDE database and related tools and resources in
1012 2019: improving support for quantification data. Nucleic Acids Res.
1013 2019;47: D442–D450. doi:10.1093/nar/gky1106

1014 60. Amulic B, Knackstedt SL, Abu Abed U, Deigendesch N, Harbort CJ, Caffrey
1015 BE, et al. Cell-Cycle Proteins Control Production of Neutrophil Extracellular
1016 Traps. Dev Cell. 2017;43: 449-462.e5. doi:10.1016/j.devcel.2017.10.013

1017 61. Sanders SA, Eisenthal R, Harrison R. NADH oxidase activity of human
1018 xanthine oxidoreductase generation of superoxide anion. Eur J Biochem.
1019 1997;245: 541–548. doi:10.1111/j.1432-1033.1997.00541.x

1020 62. Li Y, Trush MA. Diphenyleneiodonium, an NAD(P)H oxidase inhibitor, also
1021 potently inhibits mitochondrial reactive oxygen species production.
1022 Biochem Biophys Res Commun. 1998;253: 295–299.
1023 doi:10.1006/bbrc.1998.9729

1024 63. Bamberg CE, Mackay CR, Lee H, Zahra D, Jackson J, Lim YS, et al. The C5a
1025 receptor (C5aR) C5L2 is a modulator of C5aR-mediated signal transduction.
1026 J Biol Chem. 2010;285: 7633–7644. doi:10.1074/jbc.M109.092106

1027 64. Scola AM, Johswich KO, Morgan BP, Klos A, Monk PN. The human
1028 complement fragment receptor, C5L2, is a recycling decoy receptor. Mol
1029 Immunol. 2009;46: 1149–1162. doi:10.1016/j.molimm.2008.11.001

1030 65. Genestier A-L, Michallet M-C, Prévost G, Bellot G, Chalabreysse L, Peyrol S,
1031 et al. Staphylococcus aureus Panton-Valentine leukocidin directly targets
1032 mitochondria and induces Bax-independent apoptosis of human
1033 neutrophils. J Clin Invest. 2005;115: 3117–3127. doi:10.1172/JCI22684

1034 66. Majander A, Finel M, Wikström M. Diphenyleneiodonium inhibits reduction
1035 of iron-sulfur clusters in the mitochondrial NADH-ubiquinone
1036 oxidoreductase (Complex I). J Biol Chem. 1994;269: 21037–21042.
1037 doi:10.1016/s0021-9258(17)31926-9

1038 67. Galbusera C, Orth P, Fedida D, Spector T. Superoxide radical production by
1039 allopurinol and xanthine oxidase. Biochem Pharmacol. 2006;71: 1747–52.
1040 doi:10.1016/j.bcp.2006.02.008

1041 68. Metzler KD, Goosmann C, Lubojemska A, Zychlinsky A, Papayannopoulos

1042 V. Myeloperoxidase-containing complex regulates neutrophil elastase
1043 release and actin dynamics during NETosis. Cell Rep. 2014;8: 883–896.
1044 doi:10.1016/j.celrep.2014.06.044

1045 69. Petretto A, Bruschi M, Pratesi F, Croia C, Candiano G, Ghiggeri G, et al.
1046 Neutrophil extracellular traps (NET) induced by different stimuli: A
1047 comparative proteomic analysis. PLoS One. 2019;14: 1–18.
1048 doi:10.1371/journal.pone.0218946

1049 70. Fuchs TA, Brill A, Duerschmied D, Schatzberg D, Monestier M, Myers DD, et
1050 al. Extracellular DNA traps promote thrombosis. Proc Natl Acad Sci U S A.
1051 2010;107: 15880–15885. doi:10.1073/pnas.1005743107

1052 71. Kahlenberg JM, Carmona-Rivera C, Smith CK, Kaplan MJ. Neutrophil
1053 extracellular trap-associated protein activation of the NLRP3 inflammasome
1054 is enhanced in lupus macrophages. J Immunol. 2013;190: 1217–26.
1055 doi:10.4049/jimmunol.1202388

1056 72. Apel F, Andreeva L, Knackstedt LS, Streeck R, Frese CK, Goosmann C, et
1057 al. The cytosolic DNA sensor cGAS recognizes neutrophil extracellular traps.
1058 Sci Signal. 2021;14: eaax7942. doi:10.1126/scisignal.aax7942

1059

1060

1061

1062

1063
1064